AIAA JOURNAL
Vol. 39, No. 2, February 2001

# Technical Notes

*TECHNICAL NOTES are short manuscripts describing new developments or important results of a preliminary nature. These Notes cannot exceed six manuscript pages and three figures; a page of text may be substituted for a figure and vice versa. After informal review by the editors, they may be published within a few months of the date of receipt. Style requirements are the same as for regular contributions (see inside back cover).*

## Computation of Polydispersed Dusty Shock Wave Propagation

Ki-Cheol Park*
*Samsung Techwin Company, Ltd., Changwon City, Kyungnam 641-717, Republic of Korea*
and
Keun-Shik Chang†
*Korea Advanced Institute of Science and Technology, Yusung-ku, Taejeon 305-701, Republic of Korea*

### Introduction

SHOCK waves propagating in gas–particle suspension have important applications. Examples are shock waves occurring in the solid rocket plume and detonation of dusty particles by shock waves. Experimental and numerical investigations on this subject have drawn much attention. Numerically, the relaxation phenomenon of a shock wave in gas–particle suspension has been examined by Carrier,[1] Kriebel,[2] Rudinger,[3] and Marconi et al.[4] Numerical solution of the two-dimensional unsteady Euler equations was obtained by Kim and Chang[5] for the shock wave moving in gas–particle suspension over a compressible corner.

Outa et al.[6] and Sommerfeld[7] conducted shock tube experiments to study shock wave propagation in gas–particle suspension, as well as a numerical computations using the equilibrium gas approximation. Their experimental and numerical results showed a discrepancy when the incident shock Mach number was low. More recently, Sivier et al.[8] numerically simulated Sommerfeld's[7] experimental case using an unstructured adaptive grid. They[8] used the Eulerian–Eulerian approach based on the continuum assumption for both the gas and the particles. Their calculation showed some improvement over Sommerfeld's[7] earlier numerical results. However, the simulation[8] again suffered from inaccuracy in the case of low incident shock wave speed.

In the present Note, we present a new numerical method using the Lagrangian particle tracing technique and particle adaptation on an unstructured grid for the polydispersed gas–particle suspension. It is delineated why the existing numerical solution shows deviation from the experimental results of Sommerfeld.[7]

### Numerical Formulation

The two-dimensional Euler equations with particle source terms $\boldsymbol{S}$ are written in conservation form:

$$\frac{\partial \boldsymbol{U}}{\partial t} + \frac{\partial \boldsymbol{F}_i}{\partial x_i} = \boldsymbol{S} \qquad i = 1, 2 \tag{1}$$

Here $\boldsymbol{U}$ has the conservation variables and $\boldsymbol{F}$ is the flux vector. This equation is nondimensionalized using a characteristic length $L_\infty$, which is the diameter of a shock tube and the freestream properties. Roe's flux difference splitting upwind method is used to calculate the numerical fluxes. The triangular primary and polygonal dual meshes shown in Fig. 1 are the basic finite volumes, before any adaptation, employed in the present study to compute both the flux and the particle source terms. In the time direction, explicit four-stage Runge–Kutta time stepping is applied.

### Coupling Between Phases

The assumption is made that there is heat transfer but no phase change or mass transfer between the two phases. Dilute particle suspension is assumed so that collision among the droplets can be ignored. The Lagrangian particle motion is described by the ordinary differential equations

$$\frac{\mathrm{d}\boldsymbol{u}_p}{\mathrm{d}t_p} = \frac{3}{4}\frac{\rho}{\rho_p}\frac{C_D}{D_p}\Delta V \cdot L_\infty(\boldsymbol{u} - \boldsymbol{u}_p) \tag{2}$$

$$\frac{\mathrm{d}T_p}{\mathrm{d}t_p} = 6\frac{Nu}{Pr}\frac{\mu}{\rho_p}\frac{1}{\rho_\infty}\frac{L_\infty}{a_\infty}\frac{1}{D_p^2}\frac{C_{p,g}}{C_{p,p}}(T - T_p) \tag{3}$$

where

$$\Delta V = \sqrt{(u - u_p)^2 + (v - v_p)^2}$$

Here $\rho$, $T$, $u$, $v$, $a$, and $\mu$ are nondimensional density, temperature, $x$ and $y$ velocity components of the velocity vector $\boldsymbol{u}$, respectively, speed of sound, and dynamic viscosity of the gas, respectively. $D_p$ is the physical particle diameter. $C_{p,g}$ and $C_{p,p}$ are the specific heats of the gas and of the particle at constant pressure, respectively. The equations for the particle drag coefficient $C_D$ and Nussel number $Nu$ are $C_D = 112 \cdot Re_p^{-0.98}$ and $Nu = 2 + 0.6Re_p^{1/2}Pr^{1/3}$, respectively, where $Re_p = \rho|\boldsymbol{u} - \boldsymbol{u}_p|D_p/\mu$ and $Pr$ is the Prandtl number.[7] Equations (2) and (3) are analytically integrated by freezing the gas velocity and temperature at a local time step. The particle source vector $\boldsymbol{S}$ is expressed by the momentum and heat transfer terms between the phases:

$$\boldsymbol{S} = \begin{bmatrix} 0 \\ f_{PX} \\ f_{PY} \\ Q_P + u_p f_{PX} + v_p f_{PY} \end{bmatrix} \tag{4}$$

where

$$f_{PX} = (\pi/8)D_p^2\rho C_D(u_p - u)\Delta V\left(1/L_\infty^2\right)$$

$$f_{PY} = (\pi/8)D_p^2\rho C_D(v_p - v)\Delta V\left(1/L_\infty^2\right)$$

$$Q_P = \pi/(\gamma - 1)(D_p/L_\infty)(Nu/Pr)(\mu/\rho_\infty a_\infty L_\infty)(T_p - T)$$

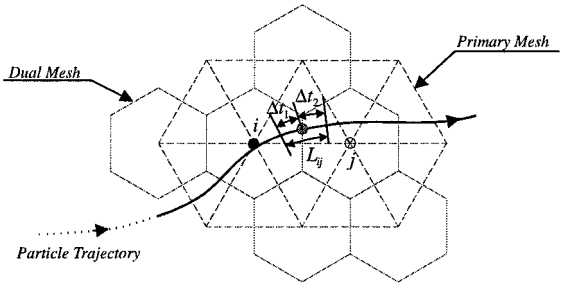


**Fig. 1 Calculation of source terms using the particle trajectory.**

Received 9 November 1999; revision received 9 August 2000; accepted for publication 31 August 2000. 

*Senior Researcher, Research Team 2, Engine Research and Development Center, 28, Sungjoo-Dong.
†Professor, Department of Aerospace Engineering, 373-1 Kusong-dong.

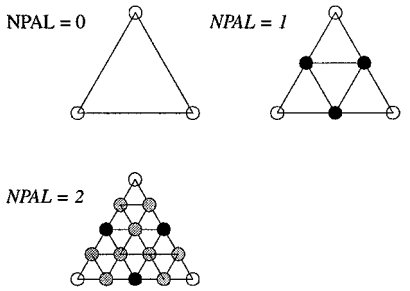


**Fig. 2 Three different levels of particle control volume.**

The source vector in the control volume $i$ of Fig. 1 is calculated at each time step by

$$S_i = \sum_{m=1}^{M} \sum_{k=1}^{K} S_{i,k}^{m} \cdot N_m \tag{5}$$

where $K$ is the total number of droplets passing through the control volume $i$ at a given time and $M$ is the total number of discretized level of the particle size. $N_m$ is the number density of the particles in the size of level $m$. When the particle crosses an intercellular boundary in a local time step, for example, the boundary between the two control volumes $i$ and $j$ in Fig. 1, the particle source vector is calculated first by accounting for the time fractions, $\Delta t_1$ and $\Delta t_2$. These are defined as the fractions of a local time step consumed in the control volumes $i$ and $j$, respectively, by the traveling particle provided that an intercellular boundary is crossed by the particle path $L_{ij}$.

## Particle Adaptation Procedure

The particle control volume is initially the same as the flow control volume. It is used to calculate the number density of the particles drifting in. Inaccuracy would result if the particle control volume were kept large while the flow control volumes are refined to small sizes when adapting to the density gradient of the gas flow. Refinement of the particle control volume is, therefore, necessary. We used one of the three particle control volumes shown in Fig. 2, which was chosen depending on the level of the flow-adaptive grid. The three cases in Fig. 2 represent no particle adaptation (NPAL = 0), light particle adaptation (NPAL = 1), and heavy particle adaptation (NPAL = 2). The circles indicate the particles representing uniform number density in the space. The number density at later times is determined by counting the number of circles that drifted into a particle control volume.

## Results and Discussion

The effect of particle adaptation is investigated using the experimental study of Sommerfeld[7]: shock Mach number $M_{s,0} = 1.49$, particle-to-gas mass loading ratio $\phi = 0.63$, and uniform particle size of diameter $D_p = 27\ \mu$m. Initially, the particle control volume is identical to the gas control volume, and uniform particle number density is assigned on the grid points. However, new grid points are generated by the flow-adaptive grids where no information about the particle number density is available. The initial particle control volumes are left relatively large because the grid is refined due to flow adaptation. As a result, the particle source terms on the old initial grid points give much more influence than the source terms on the newly generated grid points in computing the flow variables. Accordingly, the overall drag force is underpredicted, whereas the shock propagation Mach number suffers from overprediction. The shock Mach number curves in Fig. 3 show that the shock wave is decelerated by the gas–particle suspension in the shock tube. For the incident shock with $M_{s,0} = 1.49$, the dashed line represents the result of NPAL = 0; the solid line represents the case of NPAL = 2, which agrees better with the experimental results, especially in the transient region.

In the Eulerian–Eulerian approach, a mass-averaged mean particle diameter is used because the diverse particle sizes cannot be adequately treated in this method. Unfortunately, the total drag force caused by the polydispersed particles must differ from that of the uniform particles. In this paper we chose 12 different particle sizes to compute the Lagrangian motion of particle, following Sommerfeld's[7] experiment. For the incident shock Mach number $M_{s,0} = 1.26$, the result of the polydispersed particle model in Fig. 3 is in good agreement with the experiment. In contrast, the monodispersed uniform particles of the size $D_p = 27\ \mu$m gives as much deviation from the experiment as the Eulerian–Eulerian calculation made by Sivier et al.[8] does. In the case of $M_{s,0} = 1.49$, computation with the model of polydispersed particles shows about the same order of accuracy as the monodispersed case when compared with the experiment.

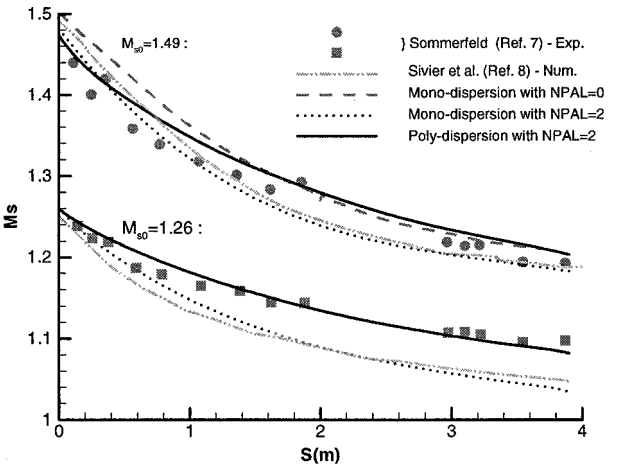


**Fig. 3 Decaying shock Mach number $M_s$ along the shock tube axis; $\phi = 0.63$.**

## Conclusions

We have developed a gas–particle two-phase flow code by adding the Lagrangian particle tracing technique to the unsteady unstructured adaptive compressible Euler formulation. It has been found that the initial particle adaptation of the particle control volume is essential to maintain the computational accuracy, provided that the adaptive grid is used for higher resolution of the shock wave. It is also shown that computation with the polydispersed particle model gives improved accuracy over the Lagrangian computation using monodispersed particles or the Eulerian–Eulerian approach using uniform particle representation.

## References

[1] Carrier, G. F., "Shock Waves in Dusty Gas," *Journal of Fluid Mechanics*, Vol. 4, Pt. 4, Aug. 1958, pp. 376–382.

[2] Kriebel, A. R., "Analysis of Normal Shock Waves in Particle Laden Gas," *Journal of Basic Engineering*, Vol. 86, Series D, No. 4, 1964, pp. 655–665.

[3] Rudinger, G., "Analysis of Nonsteady Two Phase Flow," *Physics of Fluids*, Vol. 7, No. 11, 1964, pp. 1747–1754.

[4] Marconi, F., Rudman, S., and Calia, V., "Numerical Study of One-Dimensional Unsteady Particle-Laden Flows with Shocks," *AIAA Journal*, Vol. 19, No. 10, 1981, pp. 1294–1301.

[5] Kim, S. W., and Chang, K. S., "Reflection of Shock Wave from a Compression Corner in a Particle-Laden Gas Region," *Shock Waves*, Vol. 1, No. 1, 1991, pp. 65–73.

[6] Outa, E., Tajima, K., and Morii, H., "Experiments and Analysis on Shock Waves Propagating Through a Gas-Particle Mixture," *Bulletin of the Japan Society of Mechanical Engineers*, Vol. 19, No. 130, 1976, pp. 384–394.

[7] Sommerfeld, M., "The Unsteadiness of Shock Waves Propagating Through Gas-Particle Mixtures," *Experiments in Fluids*, Vol. 3, No. 4, 1985, pp. 197–206.

[8] Sivier, M., Loth, E., Baum, J., and Löhner, R., "Unstructured Adaptive Remeshing Finite Element Method for Dusty Shock Flow," *Shock Waves*, Vol. 4, No. 1, 1994, pp. 15–23.

M. Sichel
*Associate Editor*